Photodiagnosis and Photodynamic Therapy 28 (2019) 80–87

Contents lists available at ScienceDirect

Photodiagnosis and Photodynamic Therapy

journal homepage: www.elsevier.com/locate/pdpdt

Antibacterial effect of S-Porphin sodium photodynamic therapy on *Staphylococcus aureus* and multiple drug resistance *Staphylococcus aureus*

Mengqi Jia, Bingjie Mai, Shupei Liu, Zhaozhao Li, Quanhong Liu, Pan Wang*

National Engineering Laboratory for Resource Development of Endangered Crude Drugs in Northwest China, The Key Laboratory of Medicinal Resources and Natural Pharmaceutical Chemistry, The Ministry of Education, College of Life Sciences, Shaanxi Normal University, Xi'an, Shaanxi, 710119, People's Republic of China

ARTICLE INFO

Keywords:
S-PS
aPDT
Staphylococcus aureus
Drug resistance
Biofilm
Antimicrobial Photodynamic Therapy

ABSTRACT

Background: Antibacterial photodynamic therapy (aPDT) has been proposed as an alternative strategy to inactivate bacteria. This study was designed to investigate the antibacterial effect of a novel photosensitizer S-Porphin sodium (S-PS) on plankton and biofilm cultures of *Staphylococcus aureus* (*S. aureus*) and its multiple drug resistance strain *S. aureus* (MDR *S. aureus*).

Methods: The plate counting method was used to evaluate the antimicrobial effect of S-PS-aPDT. The bacterial viability was detected by SYTO9/PI. The intracellular reactive oxygen species (ROS) generation was estimated by electron spin resonance spectroscopy and flow cytometry. The destruction of bacteria and biofilm was observed by scanning electron microscope (SEM) and atomic force microscope (AFM), respectively.

Results: The aPDT induced antibacterial effect in *S. aureus* and MDR *S. aureus* was S-PS concentration- and light dose-dependent. *S. aureus* exhibited much higher sensitivity to aPDT than MDR *S. aureus*, regarding to cell killing, ROS level, as well as morphological damages under AFM observation. When pretreated with the efflux pump inhibitors (EPIs), the intracellular uptake of S-PS in MDR *S. aureus* increased and the coupled aPDT produced significantly enhanced antibacterial efficiency.

Conclusion: S-PS-aPDT exhibited excellent bactericidal activity in plankton and biofilms. S-PS might be a good candidate for using in PDT anti-bacterial field. The introduction of EPIs could effectively improve the killing effect of MDR *S. aureus*.

1. Introduction

Staphylococcus aureus (S. aureus) is a common bacterium that causes a variety of life-threatening infections such as pneumonia, sepsis, ecthyma, impetigo, etc [1,2]. *S. aureus* has high toxicity and intrinsic multi-drug resistance, which is refractory to medical therapy.

The "antibiotic era" starts with the discovery of penicillin, streptomycin, chloramphenicol, and tetracycline [3], and all of them have saved the lives of most patients. However, with the development of modernization, the abuse of antibiotics increases the number of resistant bacteria in worldwide. According to the Centers for Disease Control and Prevention (CDC), there are at least two millions Americans suffering severe antibiotic-resistant infections each year, which result in 23,000 deaths annually [4]. There are many mechanisms for explaining bacteria resistance to antibiotics, the presence of efflux pumps and the formation of bacterial biofilm are two important factors among them. Efflux pumps belong to the transmembrane efflux systems, which serve to pump noxious compounds from microbial cell [5,6]. At present, MFS and MATE are two reported efflux pumps in MDR *S.aureus,* which depend on the changes of ion potential energy to efflux harmful substances that absorbed by MDR *S. aureus* [6,7]. Bacterial biofilm (BF) refers to the way in which bacteria adhere to the surface of non-living or active tissues and is wrapped in a heterogeneous polymeric matrix produced by themselves [8]. The main components of BF include polysaccharide intercellular adhesin (PIA), extracellular DNA (eDNA) and the like. Among them, eDNA supports the structure of biofilm, and PIA plays an adhesion role in the BF [9]. BF builds a natural barrier protecting bacteria from external stresses. So the occurrence of BF and bacterial drug-resistance account for the unsatisfactory therapeutic efficacy of clinical infections. It is a top priority that exploring new approaches to combat bacteria without producing drug-resistance.

A number of new strategies have been developed to treat bacterial infections, such as metal nanoparticles, cationic polymers, peptidoglycans, nanocarriers, photothermotherapy (PTT), and photodynamic therapy (PDT) [10]. The eradication of bacteria by PDT, called antimicrobial photodynamic therapy (aPDT), holds a special place among

* Corresponding author.
E-mail address: wangpan@snnu.edu.cn (P. Wang).

https://doi.org/10.1016/j.pdpdt.2019.08.031
Received 17 May 2019; Received in revised form 7 August 2019; Accepted 26 August 2019
Available online 27 August 2019
1572-1000/

the alternatives to antibiotics [11]. aPDT is based on the excitation of photosensitizer (PS) upon illumination and the formation of reactive oxygen species (ROS) during the process. ROS attack the cellular multiple targets including membranes, lipids, proteins, and DNA, then leading to cytoplasm leakage, degradation, and cell death [12]. The non-specific targets of ROS contribute to the advantages of aPDT, which initiate multiple death-signal pathways, producing killing effects independent of antibiotic resistance. Besides, the repetition of aPDT therapy is highly spatial-controllable without cumulative toxicity [10].

PS is an important part of aPDT. Previous studies have shown a variety of PSs with high photo-toxicity and high yield of $^1O_2$, such as 5-ALA, HPPH, PpIX, etc. [13–15]. Although some of them exhibit obvious antibacterial effects, there still exist many shortcomings, such as low water solubility, serious side effects and so on [11]. A new photosensitizer S-Porphin sodium (S-PS), was developed recently according to the optimization of HPPH (an FDA-approved PS). S-PS overcomes the poor solubility of HPPH in physiological environment and could be an ideal PS with high water solubility and low dark-toxicity [16]. Importantly, S-PS has the characteristics of high purity and easy extraction. We previously showed that S-PS exhibited significant antitumor effect under photo-stimulation [16], showing high potential photoactivity. Here, we aimed to explore the possible antibacterial effects and mechanisms of S-PS mediated aPDT (S-PS-aPDT) in *S. aureus* as well as in MDR *S. aureus,* hoping to provide evidence for using S-PS-aPDT as an alternative strategy for combating antibiotic resistance in bacterial infections (Fig. 1). Moreover, we also comparatively analyzed the possible reason for the different response efficiency between *S. aureus* and MDR *S. aureus* after the same PDT treatment. Our findings suggest that S-PS-aPDT produced significant killing effects on planktonic bacteria and biofilms of *S. aureus,* and such antibacterial efficacy in MDR *S. aureus* could be greatly enhanced by the presence of efflux pump inhibitors. We believe this work is of great importance to the indications and potent clinical applications of S-PS phototherapy.

2. Materials and methods

2.1. Bacterial strain and culture condition

S. aureus (CMCC 260003) and MDR *S. aureus* (ATCC 29213) were provided by the Shaanxi Provincial Institute of Microbiology (Xi'an, China). Both of them were stored at -80 ℃ as glycerol stocks. During resuscitation, the frozen strain was placed in water at 37 ℃ and then inoculated on Trypticase Soy Agar (TSA, Aobox biotechnology, Beijing, China). After incubation for 24 h at 37 ℃, a single colony on TSA medium was picked and cultivated overnight in Tryptica Soy Broth (TSB, Aobox biotechnology, Beijing, China). The bacterial suspension was suspended in PBS to a concentration of 2×10^8 CFU/ml prior to treatment.

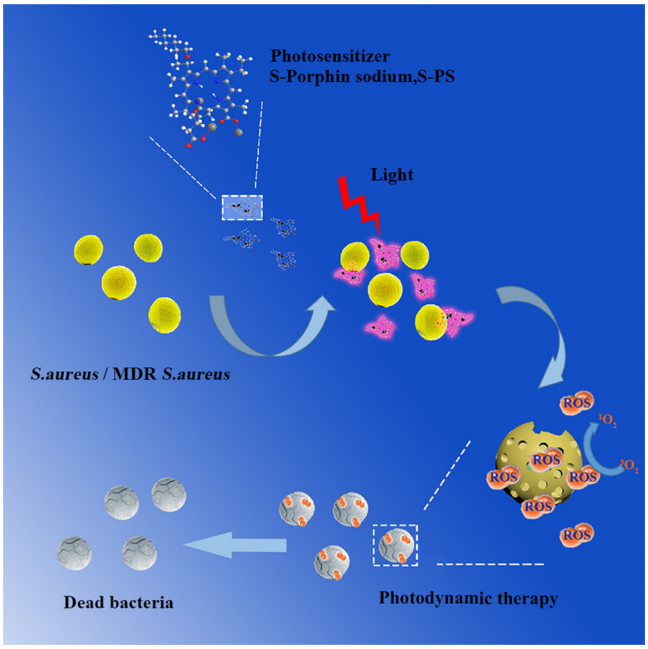

Fig. 1. Schematic diagram of S-PS combined with photodynamic therapy for killing *S. aureus*/MDR *S. aureus.*

2.2. Reagents

S-PS was kindly provided by Guilin Huiang Biochemical Pharmaceutical Co., Ltd (Guilin, China). 2′,7′-Dichlorodihydrofluorescein diacetate (H_2-DCFH-DA) and SYTO 9 fluorescent dye were obtained from Thermo Fisher Scientific (Waltham, MA, USA). Propidium iodide (PI) was obtained from the Sigma Aldrich (St Louis, MO, USA). 2, 2, 6, 6-tetramethylpiperidine (TEMPO), 5, 5-dimethyl-1-pyrroline-*N*-oxide (DMPO), reserpine, and carbonyl cyanide 3-chlorophenylhydrazine (CCCP) were purchased from Sigma Aldrich (St Louis, MO, USA).

2.3. Uptake of S-PS in S. aureus /MDR S. aureus

At first, the optimal drug uptake in bacteria was determined by alkaline lysis method according to the fluorescence intensity of S-PS. The alkaline lysis is a method for rapidly detecting drug enrichment in bacteria [17]. In brief, bacteria and S-PS (2 μg/ml) were incubated in the dark, and 1 ml sample was taken every 20 min. All samples were washed twice with PBS, centrifuged to remove the supernatant, then added buffer I (50 mM Glucose, 25 mM Tris-Hcl, 10 mM EDTA) and mixed for 2 min. After lysis Buffer II (0.2 M NaOH, 1% SDS) was added and fully mixed, samples were centrifuged for 5 min. The supernatant of each sample was added to the 96-well plate and the fluorescence was recorded by using a spectrophotometer with the excitation wavelength at 400 nm. The relative fluorescence intensity was represented as F_t (after adding S-PS at time t) minus F_0 (before adding S-PS). Next, we also visibly observed the accumulation of S-PS in *S. aureus*/MDR *S. aureus* by fluorescence microscope. Briefly, bacterial suspensions were incubated with S-PS in dark for 40 min, and washed twice with PBS, then visualized under fluorescence microscopy (Axio Imager M2; Carl Zeiss Meditec, Jena, Germany).

2.4. Photodynamic treatment

S. aureus/MDR *S. aureus* were suspended in PBS to a concentration of 2×10^8 CFU/ml, then incubated with S-PS (0.5, 1 and 2 μg/ml) at 37 ℃ in the dark. After incubated for 40 min, samples were irradiated with different doses of light (5, 10, 15 J/cm^2) with an excitation of 650 nm (NingJu photoelectric technology limited company, Xi'an, China). 1 h later, sample was diluted by gradient, and 100 μl of each was smeared on the solid agar plate and incubated for 24 h at 37 ℃. After that, the CFU (colony forming unit) was counted with at least three repeats. The S-PS alone without light exposure was used for reference.

2.5. Bacterial viability assay

In this study, the viability of *S. aureus*/MDR *S. aureus* was assessed by SYTO 9/PI double staining. SYTO 9 produces a strong green fluorescence when bound to DNA and a low intrinsic fluorescent signal when unbound [18]. PI is usually to identify dead cells with disrupted membrane. When both dyes are present, PI exhibits a stronger affinity for nucleic acids than SYTO 9, and hence, SYTO 9 is displaced by PI [19]. Therefore, the double staining of SYTO 9/PI has been used to quantify the viable and dead cells in photodynmaic antibacterial research. The bacteria were divided into six groups, including control, S-

PS alone, light alone and S-PS-aPDT group (1 μg/ml S-PS; 5, 10, 15 J/cm^2 light). After different treatment, SYTO 9/PI were added in sequence and the mixture was evenly mixed at 37 ℃ in the dark and incubated for 15 min. Samples were then detected by flow cytometry and fluorescence microscopy.

2.6. Inhibition of the bacterial efflux pumps

Efflux pump inhibitors (EPIs) have been used to increase the accumulation of antimicrobial agents in bacteria [20]. This study used two EPIs (reserpine and CCCP) to decrease the efflux of S-PS in MDR *S. aureus*. In order to explore the uptake of S-PS in MDR *S. aureus* with or without EPIs pre-incubation (20 μg/ml reserpine and 0.1 mmol/ml CCCP), alkaline lysis was performed at different time points (0, 20, 40, 60, 80, 100 min) after S-PS addition. Samples were detected as aforementioned spectrophotometry. Next, the viability of MDR *S. aureus* and *S. aureus* with or without EPIs pretreatment before aPDT was also measured by plate count assay.

2.7. Intracellular ROS level

H_2-DCFH-DA can freely traverse through the cell membrane after being incubated with bacteria. After entering the cell, H_2-DCFH-DA can be hydrolyzed into DCFH by the esterase and remained in the cell. DCFH can be oxidized to a green fluorescent substance DCF, upon excessive ROS and the fluorescence intensity of DCF is proportional to ROS production [21]. In general, *S. aureus*/ MDR *S. aureus* were incubated with 1 μg/ml S-PS for 40 min, then treated with different light doses of PDT (4, 6, 8 J/cm^2). After that, 10 mM of H_2-DCFH-DA was added to each group and incubated for 30 min. Then, samples were washed and immediately detected by flow cytometry (Novo Cyte; ACEA Biosciences, San Diego, CA, USA).

2.8. ESR detection

Free radicals have been characterized by electron spin resonance (ESR) spectroscopy coupled with spin trapping. The free radical traps commonly used in ESR are TEMPO, DMPO and so on. TEMPO mainly captures singlet oxygen [22], while DMPO can capture superoxide and hydroxyl radicals [23]. In this study, we used TEMPO and DMPO as free radical traps and performed ESR characterization on a Bruker EMX electron paramagnetic resonance spectrometer immediately post aPDT (2 μg/ml S-PS, 15 J/cm^2). As controls, the TEMPO and DMPO without light were tested for comparison.

2.9. AFM monitoring bacterial morphology

In the preparation of AFM (atomic force microscope) samples, we centrifuged the bacterial of control group and S-PS-aPDT group (2 μg/ml S-PS; 15 J/cm^2) at 9000 rpm for 5 min, then discarded the supernatant and resuspended residual bacterial in 50 μl PBS and coated them on new mica plates. The plates were fixed with 1.5% glutaraldehyde for 5 min, then washed with ultrapure water and air dried. We used tapping mode in AFM (Dimension ICON, Bruker AXS, USA) to obtain high resolution images of individual bacterial morphology before and after S-PS-aPDT. The statistic data of vertical height based on AFM analysis software (NanoScope Analysis 1.5) were also obtained as reported [24].

2.10. Photodynamic inactivation of S. aureus/MDR S.aureus biofilms

Scanning electron microscope (SEM) was used to observe the damage of *S. aureus*/MDR *S. aureus* biofilms after S-PS-aPDT. We established an *in vitro* biofilm model according to previously published methods [25,26]. Simply, *S. aureus* and MDR *S. aureus* were grown overnight on LB agar and resuspended in TSB with overnight culture. After that, 2 ml of bacteria suspension was added in the 24-well plate at a density of 2×10^8 CFU/ml in TSB, allowing bacteria further grew in the stationary plate overnight at 37 ℃. After biofilm formation, we performed aPDT treatment which divided into the control group, S-PS alone, light alone and aPDT group (10 μg/ml S-PS; 5, 10, 15 J/cm^2 light). After different treatment, the bacteria biofilm was washed with PBS and fixed with 2.5% glutaraldehyde in PBS (pH 7.2) at 4℃ for 4 h, then dehydrated with gradient ethanol (30%, 50%, 70%, 80%, 95%, 100%) for 10 min each time. Ethanol was then replaced by isoamyl acetate in different proportions. Finally, the samples were dried at the critical point, gold evaporated, and observed under a SEM (S-3400N, Hitachi, Japan).

2.11. Statistical analysis

All experiments were performed at least three times and all data are expressed as the mean ± standard deviation (SD). A value of $p < 0.05$ was considered to be significant.

3. Results

3.1. Uptake of S-PS in S. aureus / MDR S. aureus

To confirm the role of S-PS in the treatment of *S. aureus*/MDR *S. aureus*, we examined the uptake of S-PS in bacteria by fluorescence microscopy and alkaline lysis. Fig. 2A shows that under the same conditions, S-PS red fluorescence could be seen in *S. aureus* and MDR *S. aureus* after incubation for 40 min, and the former was much brighter than the later. Fig. 2B shows the fluorescence intensity of S-PS in *S. aureus* increased with incubation time and reached maximum at approximately 40 min. Similar uptake of S-PS was also found in MDR *S.*

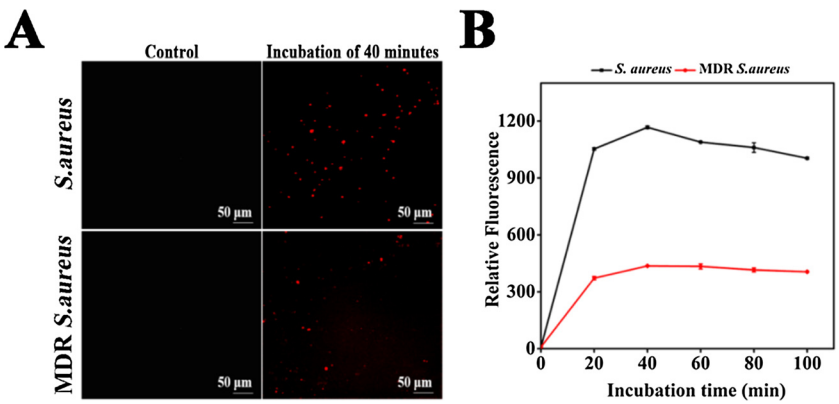

Fig. 2. Uptake of S-PS by *S. aureus*/ MDR *S.aureus*. (A) Uptake of S-PS in *S. aureus*/MDR *S.aureus* at 40 min by microscope.(B) The fluorescence intensity of S-PS in *S. aureus* and MDR *S.aureus*. Data shown are mean ± SD of three independent experiments.

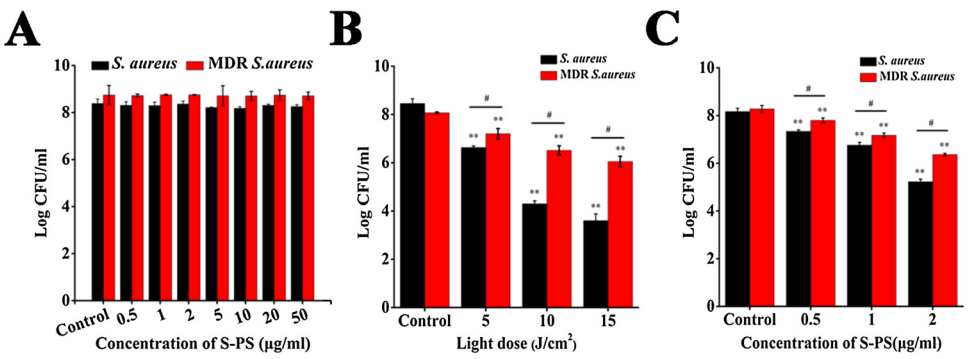

Fig. 3. The toxicity of S-PS-aPDT in bacteria. (A) Dark toxicity of S-PS on *S. aureus*/MDR *S. aureus*. The *S. aureus*/MDR *S. aureus* were incubated with different concentrations of S-PS in the dark for 6 h. (B) *S. aureus* and MDR *S. aureus* were incubated with 2 μg/ml S-PS for 40 min and exposed to different dose of light. (C) *S. aureus*/MDR *S. aureus*were incubated with different dose of S-PS and irradiated by 10 J/cm^2. Data are expressed as mean ± SD of three independent experiments. $^{**}p < 0.01$ vs Control. $^{\#}p < 0.05$, between groups.

aureus, and the uptake of S-PS in MDR *S. aureus* was 2.67-fold lower than that in *S. aureus* at 40 min.

3.2. The toxicity of S-PS-aPDT in bacteria

The dark toxicity of S-PS in *S. aureus*/MDR *S. aureus* was examined by colony counting method. It can be seen from Fig. 3A that there was no obvious damage of *S. aureus*/MDR *S. aureus* with S-PS concentrations ranging from 0.5 μg/ml to 50 μg/ml. While, the bacterial growth density gradually decreased as light dose increased, with the presence of 2 μg/ml S-PS (Fig. 3B). *S. aureus* decreased by 4.7-log under 15 J/cm^2 light compared with the initial bacterial concentration, and MDR *S. aureus* decreased by 2-log under 15 J/cm^2 light. We also studied the dose-dependence of S-PS on aPDT efficiency, which showed a positive correlation between them. In the presence of 2 μg/ml S-PS, 3.01-log of *S. aureus* viability was reduced after aPDT (10 J/cm^2), while MDR*S. aureus* decreased by 1.65-log (Fig. 3C). In a word, S-PS-aPDT has a significant antibacterial activity in *S. aureus* and MDR *S. aureus*.

3.3. Bacterial viability using SYTO 9/PI

The viability of *S. aureus* and MDR *S. aureus* after S-PS-aPDT were evaluated by SYTO 9/PI double staining. Under the fluorescence microscope, *S. aureus* in control group showed viable cells with green fluorescence and almost no red fluorescence. Compared with control, S-PS alone and light alone showed no difference, while the green fluorescence in the aPDT treated group was significantly decreased in a light dose-dependent manner. When bacteria were treated with 15 J/cm^2 light plus 1 μg/ml S-PS, almost all the cells were stained with PI with barely stained with SYTO 9. Similar phenomenon was also found in MDR *S.aureus*. Compared with *S.aureus*, it was found that the green fluorescence of MDR *S.aureus* was much more than that of *S.aureus* under the same treatment conditions (Fig. 4A). Meanwhile, the data from flow cytometry show that the red fluorescence in the treated *S. aureus*/MDR *S. aureus* increased gradually while the green fluorescence decreased gradually (Fig. 4B). The results indicate that S-PS-aPDT could damage bacteria, and the higher the irradiation dose, the more serious damage of bacteria.

3.4. Inhibition of bacterial efflux pumps in S-PS-aPDT

In order to investigate the difference between *S. aureus* and MDR *S. aureus* after S-PS-aPDT treatment, we used efflux pump inhibitors (EPIs) to suppress the efflux of S-PS in MDR *S. aureus*. It was found that the uptake of S-PS in MDR *S. aureus* was significantly increased after the addition of EPIs, which was about 1.3-folds higher than without EPIs (Fig. 5A). Moreover, the S-PS-aPDT induced antibacterial effect was obviously enhanced with the presence of EPIs in MDR *S.aureus* (Fig. 5B). However, there is no significant change in the CFU of S-PS-aPDT-treated *S. aureus* before and after adding EPIs (Fig. 5C).

3.5. Intracellular ROS generation and ESR detection

The intracellular ROS production of *S. aureus*/MDR *S. aureus* treated with aPDT was measured by flow cytometry. Fig. 6A shows the intracellular ROS levels in *S. aureus* after aPDT were significantly increased by 43.74% ($p < 0.05$), 67.04% ($p < 0.05$) and 71.11% ($p < 0.01$) when the light dose was 4, 6, and 8 J/cm^2, respectively. Similarly, the intracellular ROS production in MDR *S. aureus* after aPDT were increased by 9.23% ($p < 0.05$), 19.86% ($p < 0.05$) and 34.03% ($p < 0.01$) when the light was 4, 6, and 8 J/cm^2 (Fig. 6B). The ROS production of *S. aureus* under the same PDT conditions was significantly higher than that of MDR *S.aureus*($p < 0.01$) (Fig. 6C).

Additionally, in order to investigate the types of ROS produced by the photo-excited S-PS, ESR spectrum was scanned in S-PS solution with or without light exposure. We used TEMPO and DMPO as traps and results indicate the $^1O_2$ signal acquisition by TEMPO was very high and obvious, while the DMPO signal was relatively lower, suggesting $^1O_2$ yields during S-PS-aPDT (Fig. 7).

3.6. AFM observation of bacteria after S-PS-aPDT

To confirm the cell killing effect of S-PS-aPDT, we used AFM to observe the morphological changes of bacteria. As shown in Fig. 8, the untreated *S. aureus* and MDR *S. aureus* showed typically near-spherical structures. While, both *S. aureus* and MDR *S. aureus* after aPDT showed a clear hollow in the bacterial surface. From the processing of AFM analysis software, the surface average roughness (Ra) was significantly increased (Table 1). The above results indicate the cell wall damage and intracellular contents release after S-PS-aPDT. In addition, from the analysis of height changes, it can be seen that the damage of *S. aureus* was more serious than that of MDR *S.aureus,* the collapse depth in the former was higher than in the latter (188.936 nm vs 146.029 nm, Fig. 8).

3.7. Photodynamic inactivation of bacterial biofilms

In order to estimate the effect of S-PS-aPDT on the structure of bacterial biofilm, SEM was used to observe the morphological changes of bacterial biofilms. As shown in Fig. 9, the bacterial biofilm of the control group exhibited a dense structure in which the aggregation was stacked. The biofilm of MDR *S. aureus* showed much more dense structure than that of *S. aureus* (Fig. 9B). Nevertheless, with the increase of light dose, the structure of MDR *S. aureus/S. aureus* biofilm became gradually loose. Under a 15 J/cm^2 light with 10 μg/ml S-PS, MDR *S. aureus/S. aureus* had no typical biofilm structure and presented separately (Fig. 9). The results suggest that S-PS combined with PDT could destroy the adhesion between bacteria and had an obvious killing effect on MDR *S. aureus/S. aureus* biofilms.

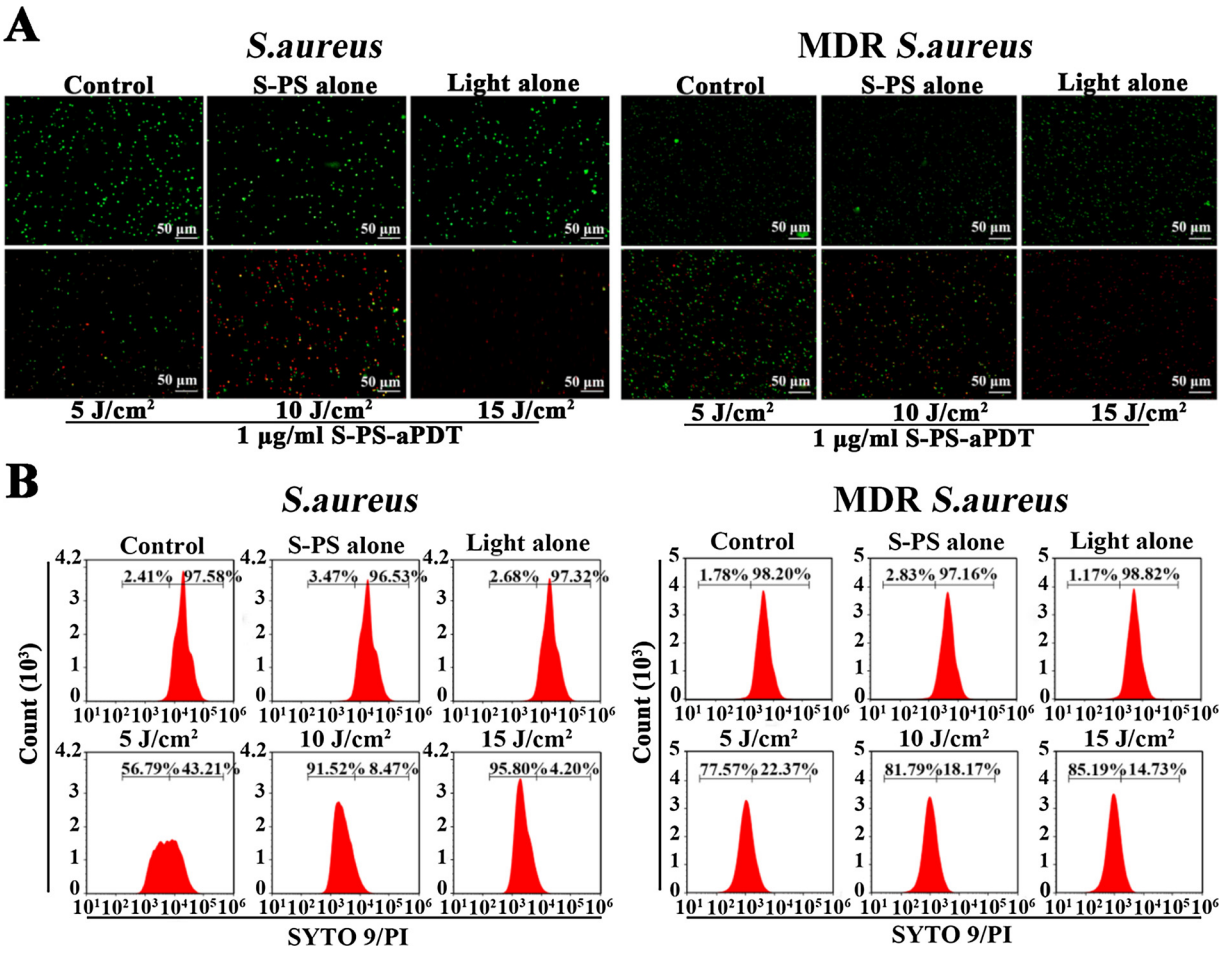

Fig. 4. Bacterial viability using SYTO 9/PI staining. (A) Fluorescence microscopy illustrated bacterial viability after different treatment. (B) Flow cytometry detected bacterial viability after different treatment. (aPDT:1 μg/ml S-PS; 5 J/cm^2, 10 J/cm^2, 15 J/cm^2 light, respectively).

4. Discussion

S.aureus has strong pathogenicity and is easily to develop drug resistance, which weaken antibiotic treatment and restrict the applications and outcomes of antibiotics [27,28]. aPDT is a promising antibacterial strategy by combination with a photosensitizer and an appropriate light exposure [29]. PS is the key factor of aPDT [30]. S-PS used in this study has been proved to be a good PS in PDT antitumor therapy [16]. However, S-PS has not been reported for bacterial infections. Therefore, the present study aimed to explore the antibacterial effects of S-PS-aPDT on *S. aureus* and MDR *S. aureus*. We demonstrated that *S. aureus*/MDR *S.aureus* could be inactivated effectively by S-PS-aPDT. S-PS had no dark toxicity and the threshold concentration of S-PS required for achieving a significant reduction in bacterial survival at light doses of 5–15 J/cm^2 was 2 μg/ml.

Meanwhile, it was found that the two strains exhibited distinct response to S-PS-aPDT treatment. The results suggest the cellular uptake of S-PS in MDR *S. aureus* was obviously lower than that in *S. aureus* (Fig. 2), which may cause the inferior PDT efficacy. Our results are consistent with others' study. It was reported that the uptake of methylene blue in multidrug resistant bacteria was lower than that in common bacteria, thus resulted in inefficient killing of resistant bacteria [31,32]. The possible explanations could be due to the high abundance of efflux pumps on the surface of MDR strains which pump toxic substances from microbial cells [33]. In order to confirm the above proposal, we added two commonly used efflux pump inhibitors

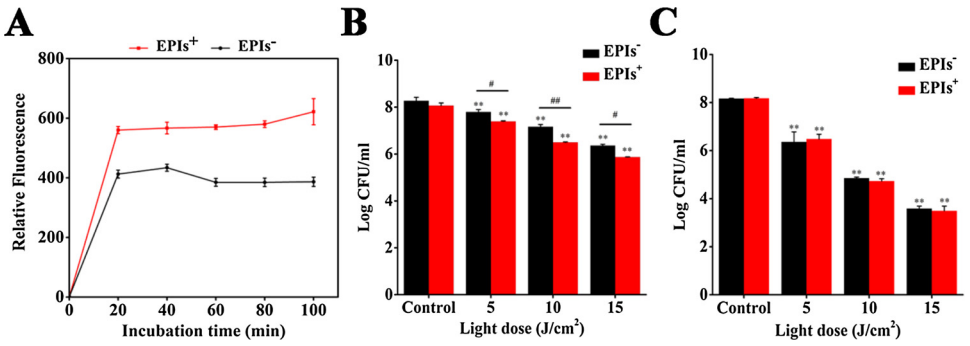

Fig. 5. Inhibition of bacterial efflux pumps in S-PS-aPDT. (A) The uptake of S-PS in MDR *S. aureus* with or without the addition of EPIs (20 μg/ml reserpine and 0.1 mmol/ml CCCP). (B) The phototoxicity of MDR *S. aureus* with or without EPIs pretreatment. MDR *S. aureus* were preincubated with EPIs and then exposed to S-PS-aPDT (2 μg/ml S-PS). (C) The phototoxicity of *S. aureus* with or without EPIs pretreatment. *S. aureus* were preincubated with EPIs, and then exposed to S-PS-aPDT (2 μg/ml S-PS). Data are expressed as mean ± SD of three independent experiments. $^{**}p < 0.01$ vs Control. $^{\#}p < 0.05$, $^{\#\#}p < 0.01$ between groups.

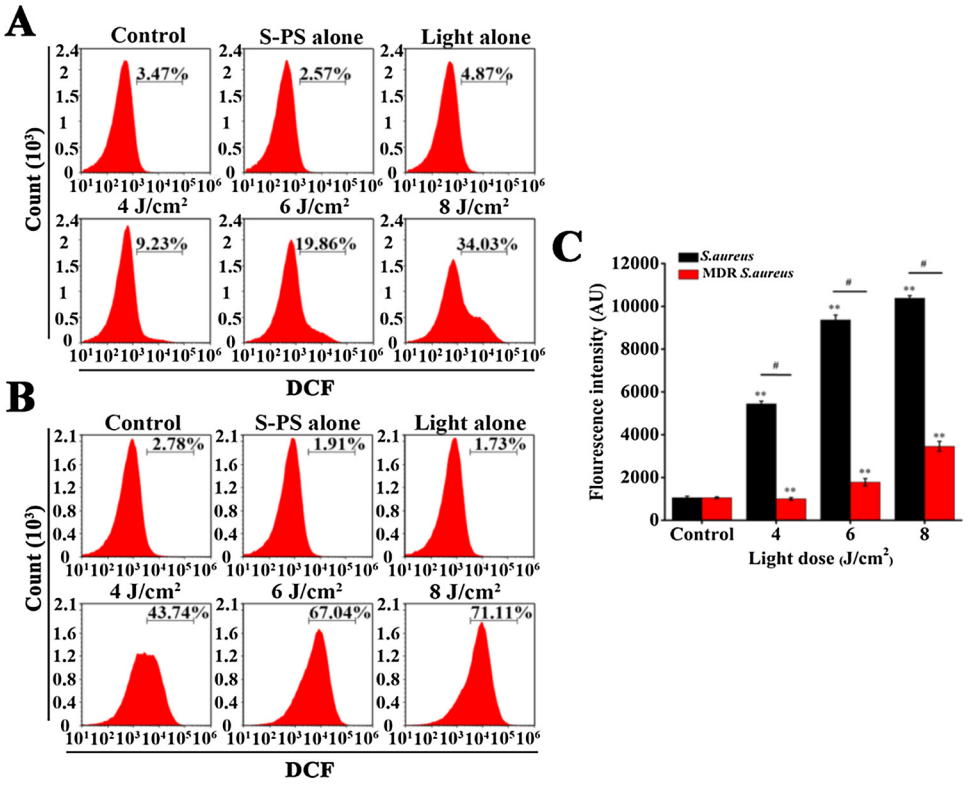

Fig. 6. Intracellular ROS generation.ROS production in *S. aureus* (A) and MDR *S. aureus* (B) was measured by flow cytometry after S-PS-PDT treatment. Bacteria were pre-incubated with H_2-DCFH-DA (10 mM) followed by illumination at different light doses in the presence of S-PS (1 μg/ml). (C) Distribution of the intensity of DCF^+ bacteria indifferent groups. Data are expressed as mean ± SD of three independent experiments. $^{**}p < 0.01$ versus Control. $^{\#}p < 0.05$, between groups.

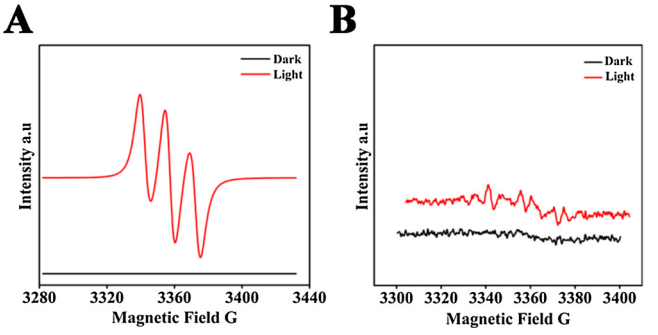

Fig. 7. ESR detection. (A) EPR spectra of TEMPO with or without 15 J/cm^2 light exposure, in the presence of 2 μg/ml S-PS (PBS as solvent, nitrogen saturated). (B) EPR spectra of DMPO with or without 15 J/cm^2 light exposure, in the presence of 2 μg/ml S-PS (PBS as solvent, nitrogen saturated).

(reserpine + CCCP) to MDR *S.aureus* before the treatment of S-PS-aPDT. The result showed that after the addition of EPIs, the uptake of S-PS by MDR *S. aureus* had a modest increase and the antibacterial effect was also significantly improved. While, the same experiment in *S. aureus* did not show any antibacterial improvement with the presence of EPIs, which may be due to the relatively low level of efflux pumps on surface of *S. aureus*. In addition, it has been reported that the drug resistance would cause the cell wall thickening, which may also hinder the penetration of S-PS in MDR *S. aureus*. Cui et al. explored the cell wall changes using transmission electron microscopy and high performance liquid chromatography, suggesting the cell wall of vancomycin-resistant *S. aureus* was significantly thicker than that of non-resistant strains [33]. Therefore, the transmembrane transportation of S-PS could be influenced by multiple factors, such as the efflux pumps, the cell wall thickness, the cell wall structures, and so on.

In order to explore the antibacterial mechanism of S-PS-aPDT, we conducted a primary evaluation on the changes of ROS level and the type of ROS. It is well known that photodynamic antibacterial therapy relies on the generation of ROS by photo-excited photosensitizes [34].

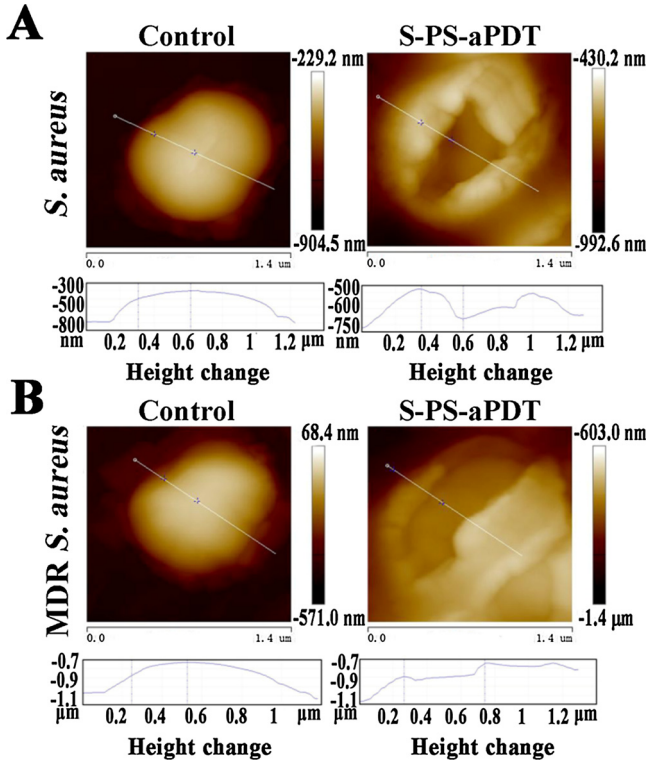

Fig. 8. AFM images of aPDT-treated *S. aureus*/MDR *S. aureus* biofilms. (A) and (B) indicate *S. aureus* and MDR *S. aureus,* respectively. Control: without any treatment; S-PS-aPDT: 2 μg/ml S-PS combined with 15 J/cm^2 light. Height changes of *S. aureus* and MDR *S. aureus* after S-PS-aPDT treatment.

The ROS generally includes superoxide anion radicals, hydroperoxides, hydrogen peroxide, hydroxyl groups, and singlet oxygen. In this study, we first examined the intracellular ROS production in *S. aureus*/MDR *S.*

Table 1
Bacterial surface roughness of *S. aureus* and MDR *S. aureus* before and after S-PS-aPDT treatment.

Groups	Rmax (nm)	Ra (nm)
S.aureus-control	23.152	4.858
S.aureus-aPDT	93.541	23.826
MDR S.aureus-control	13.504	3.266
MDR S.aureus-aPDT	19.514	7.954

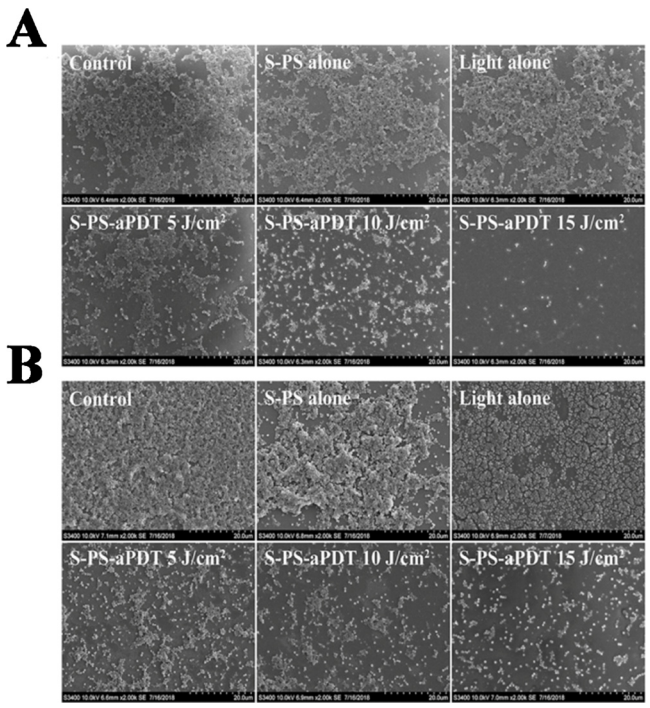

Fig. 9. SEM images of aPDT-stimulated *S. aureus*/MDR *S. aureus* biofilms. (A) and (B) indicate *S. aureus* and MDR *S. aureus,* respectively. Control = no treatment; S-PS = 10 μg/ml, light = 5 J/cm^2, 10 J/cm^2, and 15 J/cm^2.

aureus after photo-excitation. Our results indicate that the antibacterial effect of S-PS-aPDT was related to the production of ROS, which displayed S-PS- and light dose-dependence. These also agree well with the above cell uptake and viability assays. We next examined the ROS type through ESR after photo-excitation and found that the photo-excited S-PS yielded abundance of singlet oxygen and a small amount of superoxide anions. The majority singlet oxygen would be the main reason for S-PS-aPDT triggered oxidative stress in *S. aureus*/MDR *S. aureus*.

The cell wall as the first barrier for external stimuli, could be one of the targets of S-PS-aPDT. SYTO 9/PI staining suggest the integrity of bacterial membrane was disrupted after S-PS-aPDT treatment, and the severity was more prominent in *S. aureus* than that in MDR *S. aureus.* The surface morphological changes were further confirmed by AFM observation. It can be seen that the bacterial structures of *S. aureus* and MDR *S. aureus* were collapsed after S-PS-aPDT treatment, and the bacteria surface became rougher and the height was significantly reduced. The similar phenomenon has been reported by others, using AFM to evaluate the structural changes of *Enterococcus faecalis* biofilm after TBO/MB-aPDT [35]. Our results indicate that the ROS production by S-PS-aPDT can attack biomacromolecules on the cell membranes or cell walls, causing bacterial structure to collapse and cellular contents leakage as well as cell death.

Biofilms are produced in the process of bacterial culture. When the planktonic bacteria accumulate in the injured area to a certain concentration, the bacteria itself will secrete some proteins and polysaccharides to form an extracellular matrix with adhesion and protection, that is, a bacterial biofilm [36]. The dense structure of biofilm and its strong adhesion make it resistant to the invasion of foreign drugs. It usually requires 100–1000 times more antibiotics than the elimination of planktonic bacteria to damage it [37]. In recent years, it has been reported that PDT has certain inhibition on the production of bacterial biofilm [38]. In this study, we also found biofilm formation during the cultivation of bacteria, and explored the damage effect of S-PS-aPDT. Our results showed that after aPDT treatment, the adhesion between cells was reduced, and the structure of biofilm was gradually loosen and damaged. However, compared with planktonic bacteria, the bacteria survived in biofilms after S-PS-PDT were significantly higher. It is suggested that aPDT can indeed cause certain damage on bacterial biofilm, but the satisfactory killing effect cannot be achieved [39]. Dai et al. found that only 20% of the bacterial biofilm was removed after photodynamic treatment at 100 μg/ml GO [40]. The bacterial biofilm is more difficult to penetrate due to the presence of extracellular secretions, and thus cannot achieve the same effect as the killing of planktonic bacteria. Therefore, the elimination of bacterial biofilm and subsequent therapies are still worth exploring.

In general, our results demonstrate that S-PS-aPDT triggered obvious destruction on the cell wall/membrane of bacteria via ROS, significantly inhibited the proliferation of *S. aureus* and MDR *S. aureus,* in which *S. aureus* showed higher sensitivity because of the higher cellular uptake of S-PS. Besides, the antibacterial efficiency of S-PS-aPDT in MDR *S. aureus* was significantly improved after the addition of efflux pump inhibitors. Although S-PS-aPDT almost completely killed the planktonic bacteria, it couldn't eradicate the bacterial biofilm with the same dosage. Further investigations are needed to explore the increased S-PS uptake and enhanced aPDT strategies to combat biofilms, especially the MDR bacteria biofilm, to promote the application of aPDT in clinical infections.

Declaration of Competing Interest

The authors hereby declare that they have no conflict of interest.

Acknowledgments

This research was supported by the National Natural Science Foundation of China (No. 81872497), and Shaanxi Normal University Training Programs of Innovation and Entrepreneurship for Undergraduates (4560).

References

[1] B. Mai, Y. Gao, M. Li, X. Wang, K. Zhang, Q. Liu, C. Xu, P. Wang, Photodynamic antimicrobial chemotherapy for *Staphylococcus aureus* and multidrug-resistant bacterial burn infection in vitro and in vivo, Int. J. Nanomed. 12 (2017) 5915–5931, https://doi.org/10.2147/IJN.S138185.
[2] T. Horger, A. Gon, M. Schott, M. Sharan, J. Eikmeier, B. Wohlmuth, A. Zernecke, K. Ohlsen, C. Kuttler, D. Lopez, Cell differentiation defines acute and chronic infection cell types in *Staphylococcus aureus*, Elife 6 (2017) e28023, , https://doi.org/10.7554/eLife.28023.
[3] G. Dimopoulos, M.H. Kollef, J. Cohen, In 2035, will all bacteria be multiresistant? Yes, Intensive Care Med 42 (2016) 2014–2016, https://doi.org/10.1007/s00134-016-4310-y.
[4] E.J. Septimus, M.L. Schweizer, Decolonization in prevention of health care-associated infections, Clin. Microbiol. Rev. 29 (2016) 201–221, https://doi.org/10.1128/CMR.00049-15.
[5] B.D. Schindler, G.W. Kaatz, Multidrug efflux pumps of Gram-positive bacteria, Drug Resist. Updat. 27 (2016) 1–13, https://doi.org/10.1016/j.drup.2016.04.003.
[6] S. Jang, Multidrug efflux pumps in *Staphylococcus aureus* and their clinical implications, J. Microbiol. 54 (2016) 1–8, https://doi.org/10.1007/s12275-016-5159-z.
[7] S.M. Lingala, M.G.M.Mhs. Ghany, Can microbial cells develop resistance to oxidative stress in antimicrobial photodynamic inactivation? Drug Resist. Updat. 25 (2016) 289–313 doi: 110.1016/j.bbi. 2017.04.008.
[8] R.D. Wolcott, G.D. Ehrlich, Biofilms cause chronic infections, JAMA 299 (2008) 2682–2684, https://doi.org/10.1001/jama.299.22.2682.
[9] A. Di Poto, M.S. Sbarra, G. Provenza, L. Visai, P. Speziale, The effect of photodynamic treatment combined with antibiotic action or host defence mechanisms on Staphylococcus aureus biofilms, Biomaterials 30 (2009) 3158–3166, https://doi.

org/10.1016/j.biomaterials.2009.02.038.
[10] F. Xu, M. Hu, C. Liu, S.K. Choi, Yolk-structured multifunctional up-conversion nanoparticles for synergistic photodynamic-sonodynamic antibacterial resistance therapy, Biomater. Sci. 5 (2017) 678–685, https://doi.org/10.1039/c7bm00030h.
[11] F. Xiao, B. Cao, C. Wang, X. Guo, M. Li, D. Xing, X. Hu, Pathogen-specific polymeric antimicrobials with significant membrane disruption and enhanced photodynamic damage to inhibit highly opportunistic bacteria, ACS Nano 13 (2019) 1511–1525, https://doi.org/10.1021/acsnano.8b07251.
[12] H.R. Jia, Y.X. Zhu, Z. Chen, F.G. Wu, Cholesterol-assisted bacterial cell surface engineering for photodynamic inactivation of Gram-positive and Gram-negative bacteria, ACS Appl. Mater. Interfaces 9 (2017) 15943–15951, https://doi.org/10.1021/acsami.7b02562.
[13] G. Hennig, H. Stepp, A. Johansson, Photobleaching-based method to individualize irradiation time during interstitial 5-aminolevulinic acid photodynamic therapy, Photodiagnosis Photodyn. Ther. 8 (2011) 275–281, https://doi.org/10.1016/j.pdpdt.2011.03.338.
[14] A. Srivatsan, M. Ethirajan, S.K. Pandey, S. Dubey, X. Zheng, T.H. Liu, M. Shibata, J. Missert, J. Morgan, R.K. Pandey, Conjugation of cRGD peptide to chlorophyll *a* based photosensitizer (HPPH) alters its pharmacokinetics with enhanced tumor-imaging and photosensitizing (PDT) efficacy, Mol. Pharm. 8 (2011) 1186–1197, https://doi.org/10.1021/mp200018y.
[15] A. Johansson, F. Faber, G. Kniebuhler, H. Stepp, R. Egensperger, W. Beyer, F.-W. Kreth, Protoporphyrin IX fluorescence and photobleaching during interstitial photodynamic therapy of malignant gliomas for early treatment prognosis, Lasers Surg. Med. 45 (2013) 225–234, https://doi.org/10.1002/lsm.22126.
[16] X. Wang, L. Li, K. Zhang, Z. Han, Z. Ding, M. Lv, P. Wang, Q. Liu, X. Wang, Synthesis and evolution of S-Porphin sodium as a potential antitumor agent for photodynamic therapy against breast cancer, Org. Chem. Front. 6 (2018) 362–372, https://doi.org/10.1039/c8qo00959g.
[17] B. Mai, X. Wang, Q. Liu, A.W. Leung, X. Wang, C. Xu, P. Wang, The antibacterial effect of sinoporphyrin sodium photodynamic therapy on *Staphylococcus aureus* planktonic and biofilm cultures, Lasers Surg. Med. 48 (2016) 400–408, https://doi.org/10.1002/lsm.22468.
[18] P. Stiefel, S. Schmidt-Emrich, K. Maniura-Weber, Q. Ren, Critical aspects of using bacterial cellviability assays with the fluorophores SYTO9 and propidium iodide, BMC Microbiol. 15 (2015) 36, https://doi.org/10.1186/s12866-015-0376-x.
[19] S.M. Stocks, Mechanism and use of the commercially available viability stain, Baclight, Cytometry A. 61 (2004) 189–195, https://doi.org/10.1002/cyto.a.20069.
[20] N. Thota, M.V. Reddy, A. Kumar, I.A. Khan, P.L. Sangwan, N.P. Kalia, J.L. Koul, S. Koul, Substituted dihydronaphthalenes as efflux pump inhibitors of *Staphylococcus aureus*, Eur. J. Med. Chem. 45 (2010) 3607–3616, https://doi.org/10.1016/j.ejmech.2010.05.006.
[21] L. Gao, S. Shi, S. Wu, Y. Shen, S. Zhang, Y. Xiao, X. He, J. Gong, Y. Farnell, Y. Tang, Y. Huang, Iron oxide nanozyme suppresses intracellular *Salmonella* Enteritidis growth and alleviates infection*in vivo*, Theranostics 8 (2018) 6149–6162, https://doi.org/10.7150/thno.29303.
[22] J. Yin, Q. Xia, S. Cherng, I. Tang, P. Fu, G. Lin, H. Yu, D. Herreño, UVA photo-irradiation of oxygenated benz[a]anthracene and 3-methylcholanthene-generation of singlet oxygen and induction of lipid peroxidation, Int. J. Environ. Res. Public Health 5 (2008) 26–31, https://doi.org/10.3390/ijerph5010026.
[23] K. Abbas, M. Hardy, F. Poulhès, H. Karoui, P. Tordo, O. Ouari, F. Peyrot, M. Hardy, F. Poulhès, H. Karoui, P. Tordo, O. Ouari, Medium-throughput ESR detection of superoxide production in undetached adherent cells using cyclic nitrone spin traps, Free Radic. Res. 5762 (2015) 1122–1128, https://doi.org/10.3109/10715762.2015.1045504.
[24] H. Shen, E.A. López-Guerra, R. Zhu, T. Diba, Q. Zheng, S.D. Solares, J.M. Zara, D. Shuai, Y. Shen, Visible-light-responsive photocatalyst of graphitic carbon nitride for pathogenic biofilm control, ACS Appl. Mater. Interfaces 11 (2019) 373–384, https://doi.org/10.1021/acsami.8b18543.
[25] T. Xue, J. Ni, F. Shang, X. Chen, M. Zhang, Autoinducer-2 increases biofilm formation via an ica- and bhp-dependent manner in *Staphylococcus epidermidis* RP62A, Microbes Infect. 17 (2015) 345–352, https://doi.org/10.1016/j.micinf.2015.01.003.
[26] C. Sousa, P. Teixeira, R. Oliveira, The role of extracellular polymers on *Staphylococcus epidermidis* biofilm biomass and metabolic activity, J. Basic Microbiol. 49 (2009) 363–370, https://doi.org/10.1002/jobm.200800196.
[27] J. Kurlenda, M. Grinholc, Alternative therapies in *Staphylococcus aureus* diseases, Acta Biochim, Pol. 59 (2012) 171–184, https://doi.org/10.18388/abp.2012_2136.
[28] Y. Fang, T. Liu, Q. Zou, Y. Zhao, F. Wu, Water-soluble benzylidene cyclopentanone based photosensitizers for in vitro and in vivo antimicrobial photodynamic therapy, Sci. Rep. 6 (2016) 28357, https://doi.org/10.1038/srep28357.
[29] R. Abreu, M. Favarin, J. Antônio, P. De Figueiredo, F. Visioli, R. Ricci, F. Montagner, M. Vinícius, R. Só, Effectiveness of photodynamic therapy associated with irrigants over two biofilm models, Photodiagnosis Photodyn. Ther. 20 (2017) 169–174, https://doi.org/10.1016/j.pdpdt.2017.10.003.
[30] F. Heinemann, J. Karges, G. Gasser, Critical overview of the use of Ru(II) polypyridyl complexes as photosensitizers in one-photon and two-photon photodynamic therapy, Acc. Chem. Res. 50 (2017) 2727–2736, https://doi.org/10.1021/acs.accounts.7b00180.
[31] A. Rineh, N.K. Dolla, A.R. Ball, M. Magana, J.B. Bremner, M.R. Hamblin, G.P. Tegos, M.J. Kelso, Attaching the NorA efflux pump inhibitor INF55 to methylene blue enhances antimicrobial photodynamic inactivation of methicillin-resistant *Staphylococcus aureus* in vitro and in vivo, ACS Infect. Dis. 3 (2017) 756–766, https://doi.org/10.1021/acsinfecdis.7b00095.
[32] G.P. Tegos, K. Masago, F. Aziz, et al., Inhibitors of bacterial multidrug efflux pumps potentiate antimicrobial photoinactivation, Antimicrob. Agents Chemother. 52 (2008) 3202–3209, https://doi.org/10.1128/AAC.00006-08.
[33] L. Cui, X. Ma, K. Sato, K. Okuma, F.C. Tenover, E.M. Mamizuka, et al., Cell wall thickening is a common feature of vancomycin resistance in *Staphylococcus aureus*, J. Clin. Microbiol. 41 (2007) 5–14, https://doi.org/10.1128/JCM.41.1.5.
[34] H. Fan, F. Bai, D. Wang, H. Wang, Y. Zhong, Z.-Y. Qiao, D.-B. Cheng, J. Wang, L. Niu, Synthesis of self-assembled porphyrin nanoparticle photosensitizers, ACS Nano 12 (2018) 3796–3803, https://doi.org/10.1021/acsnano.8b01010.
[35] L. López-Jiménez, E. Fusté, B. Martínez-Garriga, et al., Effects of photodynamic therapy on *Enterococcus faecalis* biofilms, Lasers Med. Sci. 30 (2015) 1519–1526, https://doi.org/10.1007/s10103-015-1749-y.
[36] L. Misba, S. Zaidi, A.U. Khan, A comparison of antibacterial and antibiofilm efficacy of phenothiazinium dyes between Gram positive and Gram negative bacterial biofilm, Photodiagnosis Photodyn. Ther. 18 (2017) 24–33, https://doi.org/10.1016/j.pdpdt.2017.01.177.
[37] C.R. Arciola, D. Campoccia, P. Speziale, L. Montanaro, J.W. Costerton, Biofilm formation in *Staphylococcus* implant infections. A review of molecular mechanisms and implications for biofilm-resistant materials, Biomaterials 33 (2012) 5967–5982, https://doi.org/10.1016/j.biomaterials.2012.05.031.
[38] F.F. Sperandio, Y.-Y. Huang, M.R. Hamblin, Antimicrobial photodynamic therapy to kill Gram-negative bacteria, Recent Pat. Antiinfect. Drug Discov. 8 (2013) 108–120, https://doi.org/10.2174/1574891x113089990012.
[39] N. Venkatesan, G. Perumal, M. Doble, Bacterial resistance in biofilm-associated bacteria, Future Microbiol. 10 (2015) 1743–1750, https://doi.org/10.2217/fmb.15.69.
[40] X. Dai, Y. Zhao, Y. Yu, X. Chen, X. Wei, X. Zhang, C. Li, All-in-one NIR-activated nanoplatforms for enhanced bacterial biofilm eradication, Nanoscale 10 (2018) 18520–18530, https://doi.org/10.1039/C8NR04748K.